Eur. Phys. J. E **15**, 177–187 (2004)
DOI 10.1140/epje/i2003-10158-7

THE EUROPEAN PHYSICAL JOURNAL E

Viscoelastic phase separation in polymer blends

K. Luo[a], W. Gronski[b], and C. Friedrich

Institut für Makromolekulare Chemie and Freiburger Materialforschungszentrum, Universität Freiburg, Stefan-Meier-Str. 31, D-79104 Freiburg, Germany

Received 18 December 2003 and Received in final form 9 September 2004 /
Published online: 10 November 2004 –

Abstract. In this paper, the dynamics and morphology of viscoelastic phase separation in polymer blends is investigated based on the two-fluid model in two dimensions. At critical composition, we have carefully checked the role of shear modulus, without taking account of bulk modulus. The results show that the higher shear modulus component tends to form a dispersed phase in the intermediate stage of phase separation, if the difference between the shear moduli of the components is large enough. This is opposite to the role of bulk modulus, that the higher bulk modulus component forms a networklike pattern without taking account of the shear modulus even if it is the minority phase. The morphological formation is determined by the competition of opposite effects of shear modulus and bulk modulus. For polymer blends at critical composition, the bulk modulus difference leads to a networklike pattern formed by the higher modulus component in the intermediate stage of phase separation. But if the difference between the shear moduli of the components is large enough, a co-continuous structure is observed, resulting from the competition between shear and bulk moduli. For off-critical composition, difference in bulk modulus also leads to a networklike pattern of the component with higher bulk modulus in the intermediate stage of phase separation, but phase inversion is observed rapidly. A small difference between the shear moduli of the components can support the networklike pattern to continue for longer time. But the networklike pattern does not occur for large difference between shear moduli.

PACS. 64.75.+g Solubility, segregation, and mixing; phase separation – 83.80.Tc Polymer blends

1 Introduction

The dynamics of phase separation phenomena has been extensively studied in the past years by experimental, analytical, and numerical approaches [1–7]. In the early stage, the dynamics of phase separation is controlled by concentration fluctuation. In the late stage, the dynamics of phase separation is controlled by diffusion and surface tension. It is well established that in the late stage of phase separation domain growth satisfies the dynamical scaling law of the form $R(t) \sim t^{\alpha}$, where $R(t)$ is the average domain size at time t. The growth exponent α is an important quantity which crucially depends on the space dimension, hydrodynamic effect and composition [2–5].

Theoretically, phase separation in solids and fluids can be described by the solid model (model B) and the fluid model (model H [2]), respectively. For the former, the material diffusion completely determines the local concentration, while for the latter the local concentration can be changed by both diffusion and flow. But for polymers, viscoelasticity is one of the most significant intrinsic properties, *i.e.*, their response to deformation is intermediate between that of solids and fluids. For short times, the response is elastic and the stress is proportional to the applied strain, while in the long-time limit, a fluid-like response with stress proportional to the strain rate is observed. It is generally believed that viscoelastic effects coming from chain entanglements are important only in the very early stage, where the phase separation time is shorter than the characteristic disentanglement time of a chain [8–12]. Therefore, the theory based on model H is believed to be valid on time scales longer than the characteristic disentanglement time of a chain. This is true when components of the mixtures have the same dynamics.

However, in real systems, it may often be the case that the components of binary mixtures exhibit internal dynamic asymmetry [13]. Dynamic asymmetry may be caused by the size difference in the component molecules of a mixture, such as a polymer solution. The effect of size difference is intrinsic and ideal viscoelastic phase separation may be observed. In addition, dynamic asymmetry can also be caused by the existence of another transition, which induces slow dynamics, such as glass transition. The dynamic asymmetry leads to profound differences in the rheological properties of the components,

[a] e-mail: luokaifu@yahoo.com
[b] e-mail: gronski@makro.uni-freiburg.de

such as viscosity, elasticity and viscoelasticity. Recently, Tanaka has experimentally studied phase separation in deeply quenched polymer solutions [14,15], and polymer blends [16] quenched to a temperature near the glass transition temperature of the minority phase, respectively. The experimental results show that after an initial incubation regime, domains of less viscoelastic phase nucleate and grow up to the formation of the minority phase network, which eventually breaks down leading to phase inversion. In addition, scale invariance and self-similarity have been found to break down for viscoelastic binary fluid mixtures. Obviously, the conventional phase separation model cannot explain these experimental results.

Theoretically, there are several approaches to introduce dynamic asymmetry into the phase separation model. Jäckle *et al.* [17–19] first introduced dynamical asymmetry into the solid model to study the effects of glass transition on phase separation by incorporating a strongly concentration-dependent mobility. A similar approach was followed by Ahluwalia [20]. Clarke *et al.* [21] and Cao *et al.* [22] have investigated the viscoelastic effect on the kinetics and morphology of polymer blends through introducing a relaxing elastic term into the free-energy functional. However, including the dynamical asymmetry in the diffusion coefficient or incorporating the viscoelastic effects in the mixing free-energy function is inappropriate and not straightforward, since the relaxation nature of stress should be incorporated in a constitutive equation for mechanical stresses and the fluid nature is essential for viscoelastic phase separation. The coupling between the stress and concentration fluctuation was first noticed by de Gennes and Brochard in considering the dynamics of concentration fluctuation in polymer solutions [23,24]. Later, Helfand and Fredrickson [25] applied a dynamic coupling mechanism to polymer solutions under shear flow. Then, Onuki [26], Onuki and Doi [27], and Milner [28] developed a two-fluid model, which considers two different velocities for the two components. The first simulation based on the two-fluid model for polymer solutions was performed by Taniguchi and Onuki [29]. However, the two-fluid model incorporating dynamical asymmetry due to asymmetric distribution of bulk stresses [13,30–34] has successfully explained many features of the viscoelastic phase separation experiments, such as the formation of transient network and eventual phase inversion. Tanaka and Araki's simulation results for the viscoelastic phase separation in off-critical polymer solutions [30,31], show that bulk stress should be responsible for the suppression of the homogeneous growth of concentration fluctuations, the volume shrinking of the polymer-rich phase and the phase inversion in the final stage, while the shear stress is responsible for the network pattern with threadlike structure. Recently, the two-fluid model has also been applied to viscoelastic microphase separation in diblock copolymers [35].

However, to the best of our knowledge, the dynamics and morphology of viscoelastic phase separation in polymer blends is still not clear. Compared with polymer solutions, viscoelastic phase separation in polymer blends is more complicated because for polymer solutions, the stress only acts on the polymer, not on the solvent, while for polymer blends the stress acts on the two components. In addition, in previous studies for polymer solutions [30, 31], the effect of the shear modulus on viscoelastic phase separation is investigated far from the critical composition, and the results show that the shear modulus almost does not change the morphology of phase separation. We argue that the effect of shear modulus on the morphological evolution may become obvious at the critical composition. In this paper, we use the two-fluid model to study the phase separation for polymer blends in two dimensions that is characterized by a strong asymmetry between the viscoelastic moduli of the two components. We focus our attention on the role of shear and bulk stress in the morphology formation.

2 Two-fluid model and simulation algorithm

First, we describe the basic equations of viscoelastic phase separation for polymer blends. They are based on the two-fluid model derived from Onuki [26], Onuki and Doi [27], and further developed by Tanaka [30–33]. Let $\phi_A(\mathbf{r}, t)$ and $\phi_B(\mathbf{r}, t)$ be the volume fractions of components A and B at a point $\mathbf{r}$ and time t, and define $\mathbf{v}_A(\mathbf{r}, t)$ and $\mathbf{v}_B(\mathbf{r}, t)$ to be their velocities, respectively. For clarity, in the following we use ϕ and $(1-\phi)$ instead of $\phi_A(\mathbf{r}, t)$ and $\phi_B(\mathbf{r}, t)$, respectively. Assuming, for simplicity, that the two components have the same density, the basic equations are given by

$$\frac{\partial \phi}{\partial t} = -\nabla \cdot (\phi \mathbf{v}_A) = -\nabla \cdot (\phi \mathbf{v}) - \nabla \cdot [\phi (1-\phi)(\mathbf{v}_A - \mathbf{v}_B)], \tag{1}$$

$$\mathbf{v}_A - \mathbf{v}_B = -\frac{(1-\phi)}{\zeta}\left[\phi \nabla \frac{\delta F}{\delta \phi} - \nabla \cdot \boldsymbol{\sigma}^A + \frac{\phi}{1-\phi}\nabla \cdot \boldsymbol{\sigma}^B\right], \tag{2}$$

$$\rho \frac{\partial \mathbf{v}}{\partial t} \cong -\phi \nabla \frac{\delta F}{\delta \phi} + \nabla p + \nabla \cdot \boldsymbol{\sigma}^A + \nabla \cdot \boldsymbol{\sigma}^B, \tag{3}$$

where ζ is the friction coefficient, $\boldsymbol{\sigma}^A$ and $\boldsymbol{\sigma}^B$ are the viscoelastic stresses acting on components A and B, respectively, and F is the mixing free-energy functional of the system. Here, the volume average velocity is given by $\mathbf{v}(\mathbf{r}, t) = \phi_A(\mathbf{r}, t)\mathbf{v}_A(\mathbf{r}, t) + \phi_B(\mathbf{r}, t)\mathbf{v}_B(\mathbf{r}, t)$. P is the pressure, which is determined to satisfy the incompressible condition $\nabla \cdot \mathbf{v} = 0$. Here, we should note that for polymer solutions, the viscoelastic stress only acts on the polymer and not directly on the solvent. So, if we set $\nabla \cdot \boldsymbol{\sigma}^B = 0$ in equation (2) and $\nabla \cdot \boldsymbol{\sigma}^B = \eta_s \nabla^2 \mathbf{v}$ in equation (3), where η_s is the solvent viscosity, the two-fluid model for polymer solutions is recovered.

The mixing free-energy functional is given by $F = \int \mathrm{d}\mathbf{r}\left\{ f(\phi(\mathbf{r})) + D|\nabla \phi(\mathbf{r})|^2/2 \right\}$, where D is the interfacial tension coefficient, and $f(\phi_A)$ is the free-energy per unit volume of a mixture. Here, we use the Flory-Huggins free energy [36]: $f(\phi)/k_B T = (1/N_A)\phi \ln \phi + (1/N_B)(1-\phi)\ln(1-\phi) + \chi\phi(1-\phi)$, where N_A and N_B

are the degree of polymerization of the polymers A and B, χ is the Flory-Huggins interaction parameter, k_{B} is Boltzmann's constant, T is the temperature.

The stress tensor is defined as [30–32,34,35]

$$\sigma_{ij}^{\beta} = \int \mathrm{d}t' \Bigg[G_{\beta}(t-t') \left(\frac{\partial v_{\beta}^{j}}{\partial x_i} + \frac{\partial v_{\beta}^{i}}{\partial x_j} - \frac{2}{d} (\nabla \cdot \mathbf{v}_{\beta}) \delta_{ij} \right) + K_{\beta}(t-t') (\nabla \cdot \mathbf{v}_{\beta}) \delta_{ij} \Bigg], \quad (4)$$

where $\beta = A$ or B, d is the spatial dimensionality, and G and K are the shear and bulk relaxation moduli, respectively. In our simulation, we assume the Maxwell-type relaxation for both shear and bulk relaxation moduli with a single relaxation time, for simplicity:

$$G_{\beta}(t) = M_{\beta \mathrm{s}} \exp(-t/\tau_{\beta \mathrm{s}}), \quad K_{\beta}(t) = M_{\beta \mathrm{b}} \exp(-t/\tau_{\beta \mathrm{b}}). \quad (5)$$

Here, $M_{\beta \mathrm{s}}$, $M_{\beta \mathrm{b}}$, $\tau_{\beta \mathrm{s}}$, and $\tau_{\beta \mathrm{b}}$ are functions of $\phi_{\beta}(\mathbf{r})$ [30–34], *i.e.*,

$$M_{\beta \mathrm{s}} = M_{\beta \mathrm{s}}^{0} \phi_{\beta}^{2}, \qquad \tau_{\beta \mathrm{s}} = \tau_{\beta \mathrm{s}}^{0} \phi_{\beta}^{2},$$
$$M_{\beta \mathrm{b}} = M_{\beta \mathrm{b}}^{0} \theta(\phi_{\beta} - \phi_{\beta}^{0}), \quad \tau_{\beta \mathrm{b}} = \tau_{\beta \mathrm{b}}^{0} \phi_{\beta}^{2}, \quad (6)$$

where ϕ_{β}^{0} is the average composition of polymers A and B, $\theta\left(\phi_{\beta} - \phi_{\beta}^{0}\right)$ is the step function that equals 1.0 when ϕ_{β} is larger than ϕ_{β}^{0} while it equals zero when ϕ_{β} is smaller than ϕ_{β}^{0}.

In the simulation, we solve the following equations instead of equation (4) [30–35]:

$$\frac{\partial \boldsymbol{\sigma}_{\beta \mathrm{s}}}{\partial t} + \mathbf{v}_{\beta} \cdot \nabla \boldsymbol{\sigma}_{\beta \mathrm{s}} = \boldsymbol{\sigma}_{\beta \mathrm{s}} \cdot \nabla \mathbf{v}_{\beta} + (\nabla \mathbf{v}_{\beta})^{T} \cdot \boldsymbol{\sigma}_{\beta \mathrm{s}} - \frac{\boldsymbol{\sigma}_{\beta \mathrm{s}}}{\tau_{\beta \mathrm{s}}(\phi)} + M_{\beta \mathrm{s}}(\phi) \left(\nabla \mathbf{v}_{\beta} + (\nabla \mathbf{v}_{\beta})^{T} \right), \quad (7)$$

$$\frac{\partial \sigma_{\beta \mathrm{b}}}{\partial t} + \mathbf{v}_{\beta} \cdot \nabla \sigma_{\beta \mathrm{b}} = -\frac{\sigma_{\beta \mathrm{b}}}{\tau_{\beta \mathrm{b}}(\phi_{\beta})} + M_{\beta \mathrm{b}}(\phi_{\beta}) \nabla \cdot \mathbf{v}_{\beta}. \quad (8)$$

Since the shear stress is a traceless tensor, we calculate the final form of the shear stress as $\boldsymbol{\sigma}_{\beta \mathrm{s}}^{\mathrm{f}} = \boldsymbol{\sigma}_{\beta \mathrm{s}} - \frac{1}{d} \mathrm{Tr}(\boldsymbol{\sigma}_{\beta \mathrm{s}}) \mathbf{I}$, where $\mathbf{I}$ is a unit tensor. Hereafter, we denote this final stress $\boldsymbol{\sigma}_{\beta \mathrm{s}}^{\mathrm{f}}$ as $\boldsymbol{\sigma}_{\beta \mathrm{s}}$. The bulk stress is isotropic in equation (8), it is expressed by a scalar variable. Therefore, we have $\boldsymbol{\sigma}_{\beta \mathrm{b}} = \sigma_{\beta \mathrm{b}} \mathbf{I}$. So the total stress supported by the component β is expressed as $\boldsymbol{\sigma}^{\beta} = \boldsymbol{\sigma}_{\beta \mathrm{s}} + \boldsymbol{\sigma}_{\beta \mathrm{b}}$.

The above equations are solved numerically by the Euler method in two dimensions using periodic boundary conditions. The lattice size is 128×128. The grid size and time step are chosen as $\Delta x = \Delta y = 1$, $\Delta t = 0.02$ to ensure the stability. The velocity field $\mathbf{v}$ is solved in Fourier space ($\mathbf{k}$ space) under incompressible conditions as follows: $\rho \frac{\partial \mathbf{v}(\mathbf{k},t)}{\partial t} = \left(\mathbf{I} - \frac{\mathbf{k}\mathbf{k}}{k^2}\right) \cdot \left[-\phi \nabla \frac{\delta F}{\delta \phi} + \nabla \cdot \boldsymbol{\sigma}^{A} + \nabla \cdot \boldsymbol{\sigma}^{B} \right]_{k}$, where $[\cdots]_{k}$ means the Fourier transform. For simplicity, we set $N_A = N_B = 1$, $k_{\mathrm{B}}T = 1.3$, $\zeta = 0.1$, $\chi = 2.7$, $D = 1.0$. A Gaussian random noise with an intensity of 0.001 was superimposed on a specified initial uniform composition $\bar{\phi}_A$.

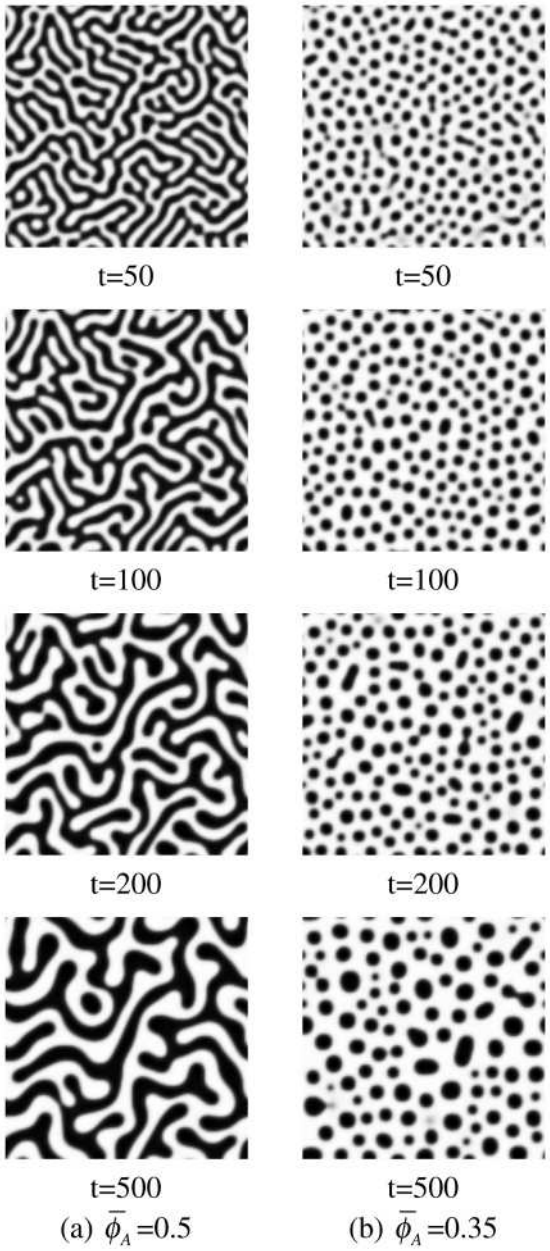

Fig. 1. Time evolution of phase-separating domains of polymer blends without viscoelasticity for mixtures (a) $\bar{\phi}_A = 0.5$ and (b) $\bar{\phi}_A = 0.35$. A-rich regions and B-rich regions are represented by black and white, respectively.

3 Simulation results and discussion

If we assume dynamic symmetry and $\mathbf{v} = 0$, the two-fluid model reduces to the solid model (model B): $\frac{\partial \phi}{\partial t} = \nabla \cdot \frac{\phi(1-\phi)^2}{\zeta} \nabla \frac{\delta F}{\delta \phi}$. For comparison, we first show the pattern evolution of phase-separating polymer blends without viscoelastic effect for both the critical composition $\bar{\phi}_A = 0.5$ and the off-critical composition $\bar{\phi}_A = 0.35$, as shown in Figures 1a and b, respectively. Homogenous

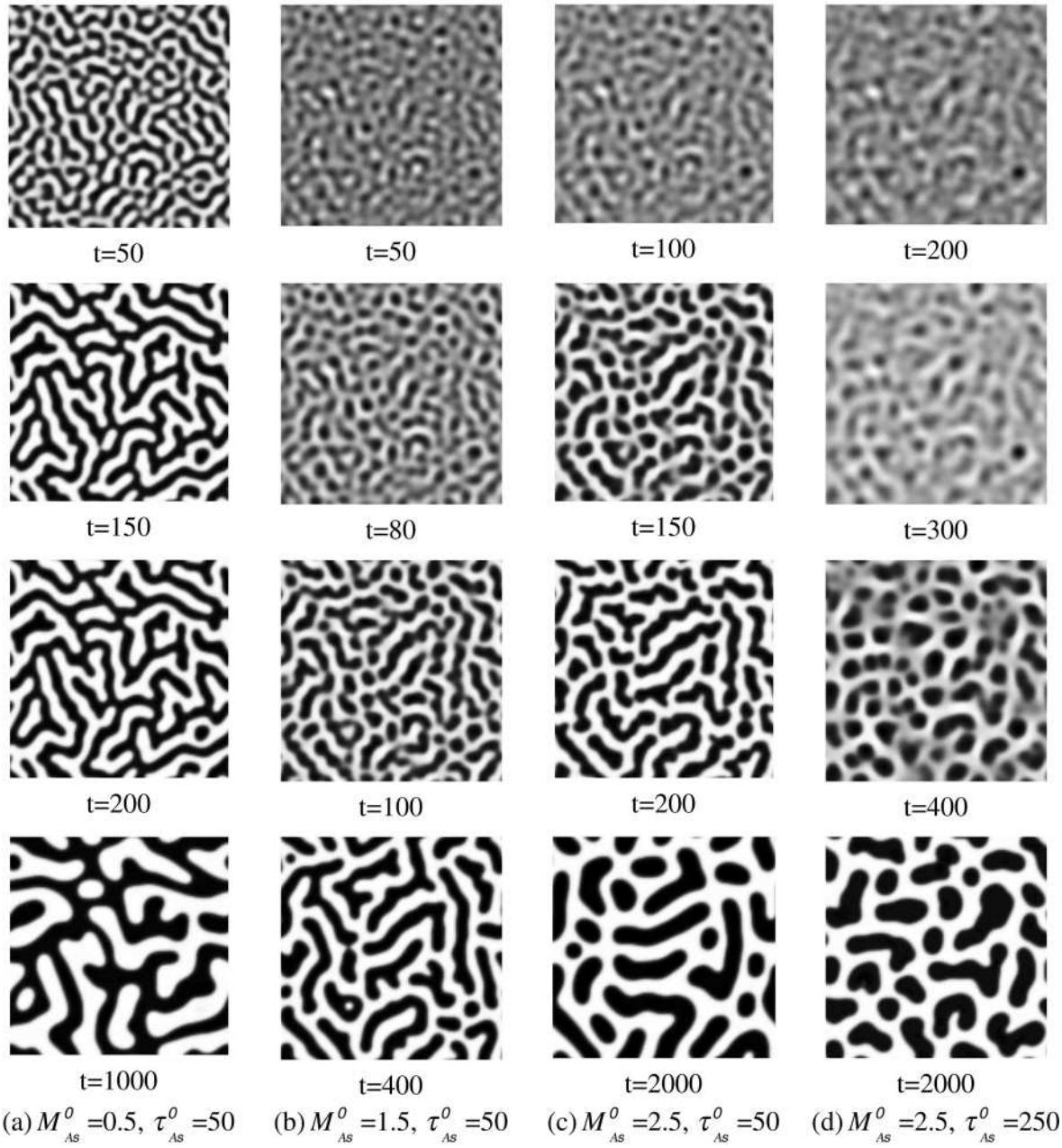

Fig. 2. Time evolution of phase-separating domains of polymer blends with shear modulus and without bulk modulus for critical mixtures $\bar{\phi}_A = 0.5$. The parameters are set as $M^0_{Bs} = 0.5$, $\tau^0_{Bs} = 50$ and (a) $M^0_{As} = 0.5$, $\tau^0_{As} = 50$, (b) $M^0_{As} = 1.5$, $\tau^0_{As} = 50$, (c) $M^0_{As} = 2.5$, $\tau^0_{As} = 50$, (d) $M^0_{As} = 2.5$, $\tau^0_{As} = 250$. A-rich regions and B-rich regions are represented by black and white, respectively.

binary mixtures segregate into two phases with different compositions when quenched into thermodynamically unstable regions of their phase diagram. For critical mixtures, these phases form interconnected domains (Fig. 1a), which produce a co-continuous structure with sharp, well-developed interfaces in the late stage of phase separation. For off-critical mixtures, these phases form a so-called droplet phase, which in turn undergoes subsequent coarsening via coalescence, as shown in Figure 1b. The domains grow with time, and the length scale of the phase separation changes from a microscopic molecular scale in the very early times to a macroscopic scale in the final stages of this process. In the early stage the dynamics of phase separation is governed by concentration fluctuation. However, in the late stage, the dynamics of phase separation is controlled by diffusion and surface tension and domain growth satisfies the dynamical scaling law of the form $R(t) \sim t^{1/4}$. For the solid model (model B) with constant mobility, the coarsening is controlled by bulk diffusion. It is well established that, in the late stages, the growth exponent is 1/3, which satisfies the Lifshitz-Slyozov scaling law [5]. But for a variable mobility, such as in our case,

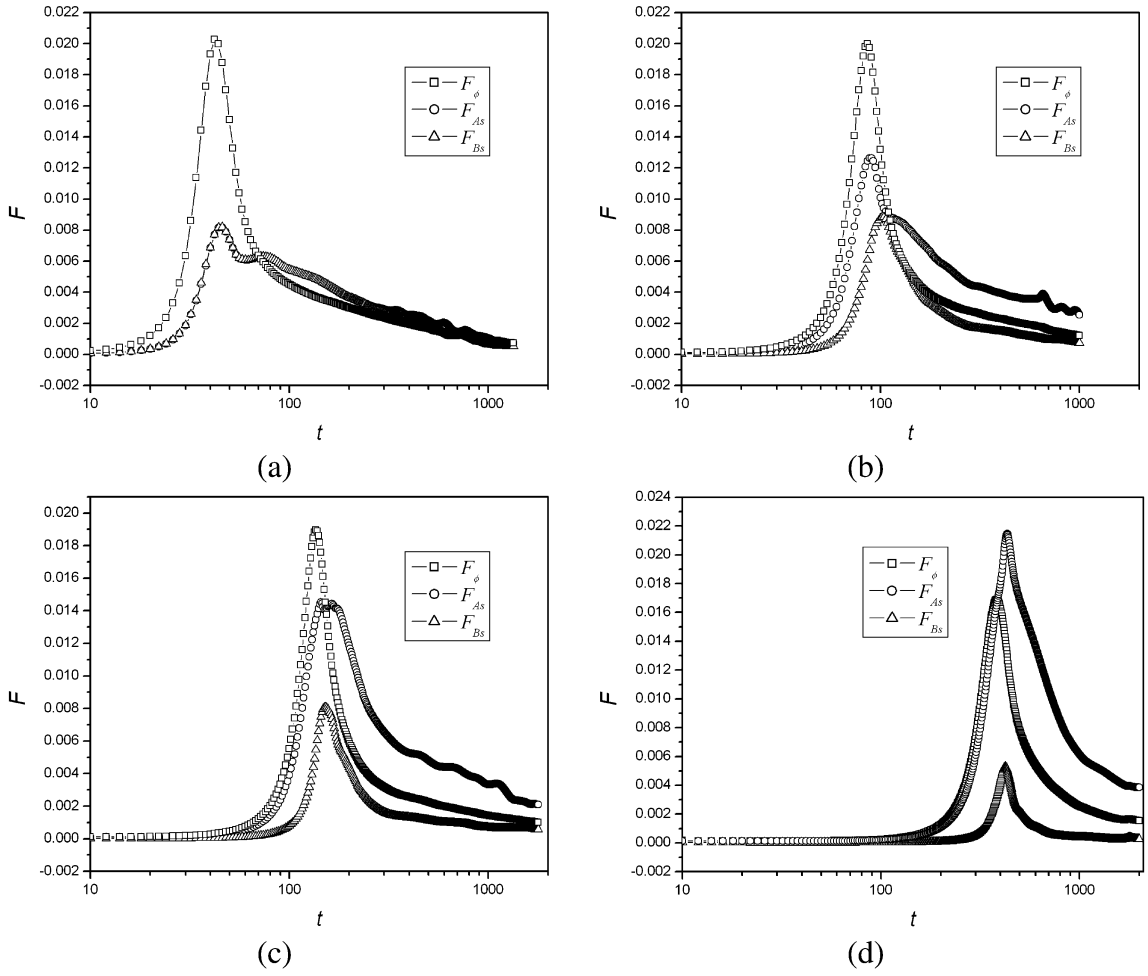

Fig. 3. Time evolution in the average magnitudes of thermodynamic and shear mechanical forces for the cases depicted in Figure 2 (a), (b), (c) and (d).

the mobility depends on local composition, $\phi(1-\phi)^2/\xi$, the interface-diffusion–controlled coarsening leads to 1/4 exponent [37].

In the following let us take account of the cases with viscoelastic effect. To understand the dynamics of viscoelastic phase separation more clearly, the temporal changes in the average magnitude per lattice of the five forces are investigated, namely, thermodynamic force $\phi(1-\phi)\nabla(\delta F/\delta\phi)$, the shear mechanical forces acting on polymer A, $-(1-\phi)\nabla\cdot\boldsymbol{\sigma}_{A\mathrm{s}}$, and on polymer B as well, $\phi\nabla\cdot\boldsymbol{\sigma}_{B\mathrm{s}}$, and the bulk mechanical forces acting on A, $-(1-\phi)\nabla\cdot\boldsymbol{\sigma}_{A\mathrm{b}}$, and on polymer B as well, $\phi\nabla\cdot\boldsymbol{\sigma}_{B\mathrm{b}}$. We define $F_\phi = |\phi(1-\phi)\nabla(\delta F/\delta\phi)|$, $F_{A\mathrm{s}} = |-(1-\phi)\nabla\cdot\boldsymbol{\sigma}_{A\mathrm{s}}|$, $F_{A\mathrm{b}} = |-(1-\phi)\nabla\cdot\boldsymbol{\sigma}_{A\mathrm{b}}|$, $F_{B\mathrm{s}} = |\phi\nabla\cdot\boldsymbol{\sigma}_{B\mathrm{s}}|$ and $F_{B\mathrm{b}} = |\phi\nabla\cdot\boldsymbol{\sigma}_{B\mathrm{b}}|$.

3.1 Case of $\bar{\phi}_A = 0.5$

First, let us focus our attention on the role of the shear relaxation modulus. In Tanaka and Araki's simulations [31], for the case without bulk modulus but with shear modulus, the morphological evolution is almost the same as usual phase separation. We think that it is reasonable because the composition of the polymer is 0.35, which is far from the critical composition, and the shear modulus is not large enough to affect the morphology. But for the case of critical composition, the effect of shear modulus on morphological evolution may be obvious.

Figures 2a, b and c show the morphological evolution without bulk modulus but with different shear modulus $M^0_{A\mathrm{s}}$. The shear relaxation time for the component A is set as $\tau^0_{A\mathrm{s}} = 50$. The parameters for the component B are set as $M^0_{B\mathrm{s}} = 0.5$, and $\tau^0_{B\mathrm{s}} = 50$. For $M^0_{A\mathrm{s}} = 0.5$, *i.e.*, where there is no difference between the moduli of the two components, compared with Figure 1a, the morphological difference is not obvious, as shown in Figure 2a. But for higher $M^0_{A\mathrm{s}}$, *i.e.*, $M^0_{A\mathrm{s}} = 1.5$ and 2.5, the phase separation is retarded and in the early stage of phase separation, *i.e.*, $t = 80$ for $M^0_{A\mathrm{s}} = 1.5$ and $t = 150$ for $M^0_{A\mathrm{s}} = 2.5$, the higher shear modulus A-rich phase forms obviously dispersed droplets and cylinders in the matrix of the lower shear modulus B-rich phase, as shown in Figures 2b and c. For $M^0_{A\mathrm{s}} = 2.5$, the dispersed morphology can continue for extremely long time, *i.e.*, $t = 2000$. If we fix $M^0_{A\mathrm{s}} = 2.5$ and

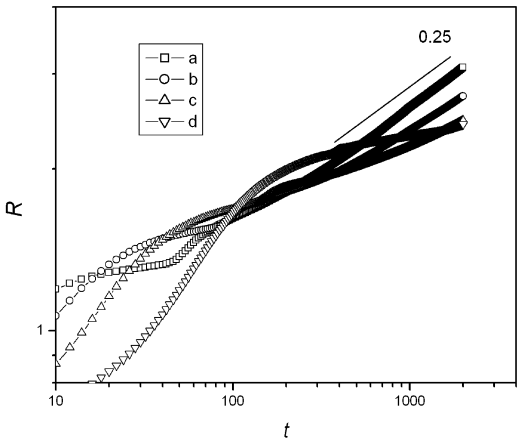

Fig. 4. Time evolution of the average domain size for the cases depicted in Figure 2 (a), (b), (c) and (d).

further increase the relaxation of time of component A, *i.e.*, $\tau^0_{A\mathrm{s}} = 250$, the phase separation is further delayed and the dispersed morphology is clearer, as shown in Figure 2d.

The time evolution of thermodynamic and shear mechanical forces are shown in Figure 3. It can be seen that for all cases the three forces have only one maximum, revealing the coupling between diffusion field and stress field. The different peak positions indicate the different extents to which the shear relaxation modulus suppresses the initial rapid increase in concentration fluctuation. With increase of the difference between the shear moduli and/or relaxation times, the peak positions are at longer time, indicating that phase separation is retarded. For the case without difference between shear moduli, shear mechanical forces acting on the two components are equal (Fig. 3a). In addition, the difference between shear mechanical forces increases with the increase of the difference between shear moduli and/or relaxation times. Three important features for the large difference between shear moduli of the components are, as shown in Figures 3c and d, 1) in the early stage of phase separation, the shear mechanical force mainly acts on the higher shear modulus A-rich phase, and the difference between thermodynamic force and shear mechanical force acting on the higher shear modulus A-rich phase is very small; 2) the peak position of the shear mechanical forces is retarded compared with that of the thermodynamic force; 3) in the late stage, the shear stress acting on the higher shear modulus A-rich phase is much larger than that acting on the B-rich phase. These factors lead to the formation of the dispersed phase of the higher shear modulus A-rich phase.

Figure 4 shows the time evolution of the domain size for all the four cases in Figure 2. It can be seen that the domain growth is slowed down with increase of the difference between shear moduli and/or relaxation times, which indicates that dynamical universality is broken down by the different viscoelasticity of the two components.

Figure 5 shows the morphological evolution with bulk modulus. The parameters are set as $M^0_{A\mathrm{b}} = 2.5$, $M^0_{B\mathrm{b}} = 0.5$, $\tau^0_{A\mathrm{s}} = 50$; $\tau^0_{B\mathrm{s}} = 50$, $\tau^0_{A\mathrm{b}} = 10$ and $\tau^0_{B\mathrm{b}} = 10$. For the case without shear stress, the domains of the lower bulk modulus B-rich phase nucleate, grow up and seldom merge together, leading to the formation of the higher bulk modulus A-rich phase network, *e.g.*, $t = 100$, as shown in Figure 5a. Later the higher bulk modulus A-rich phase network partly breaks down rapidly, resulting from the rapid merging of the lower bulk modulus B-rich droplets. At the same time, the growth of the domain is very fast. However, the system does not relax to co-continuous structure. In the late stage of phase separation, the more viscoelastic phase still forms a matrix and the less viscoelastic phase forms droplets. Compared with Figures 2c and d, it is very clear that the shear relaxation modulus and the bulk relaxation modulus play a completely different role in the morphological formation: for the more viscoelastic component, the former leads to the formation of dispersed phase; on the contrary, the latter induces the formation of a matrix. For the cases with shear modulus (Figs. 5a, b and c), the phase separation is delayed and it is also related to the difference between the shear moduli of the components. For the case without difference between the shear moduli of the two components $M^0_{A\mathrm{s}} = 0.5$, $M^0_{B\mathrm{s}} = 0.5$, the lower bulk modulus B-rich phase is also dispersed as isolated droplet in the matrix of the higher bulk modulus A-rich phase in the early stage of phase separation (Fig. 5b). But in the late stage of phase separation, the B-rich phase keeps the dispersed phase, and almost no merging between domains occurs. The domain growth is slower than that for the case without shear modulus. When $M^0_{A\mathrm{s}} = 1.0$, $M^0_{B\mathrm{s}} = 0.5$, *i.e.*, where there is a small difference between the shear moduli of two components, the morphology is almost the same as the case with the same shear moduli, as shown in Figure 5c. However, if we further increase the difference between the shear moduli, such as $M^0_{A\mathrm{s}} = 2.5$, $M^0_{B\mathrm{s}} = 0.5$, the morphology is completely different, see Figure 5d. The lower bulk modulus B-rich phase does not form an isolated droplet in the early stage of phase separation. It seems that the isolated droplets are easy to be deformed and merge with each other due to the large difference between shear stresses of two components, resulting in only co-continuous structure. It can also be seen that the interface is not smooth, indicating the effect of shear stress. Different pattern selection mechanisms between shear modulus and bulk modulus lead to cancel the opposite effects, and this is in favour of co-continuous structure.

To clearly understand the morphological development with the bulk modulus, we investigate the time evolution of forces, as shown in Figures 6a, b, c and d. The regimes prior to the force maxima correspond to the early stage of phase separation, which indicates that the system is in a "frozen" state, the concentration fluctuation accelerates during the intermediate period, and gradually approaches a maximum with the attenuation of the driving force. The higher bulk modulus A-rich phase bears larger bulk stress. Correspondingly, the shear mechanical force acting on the higher shear modulus A-rich phase is also larger and phase separation is delayed with the increase of the difference between the shear moduli. From Figure 6b, it can be seen

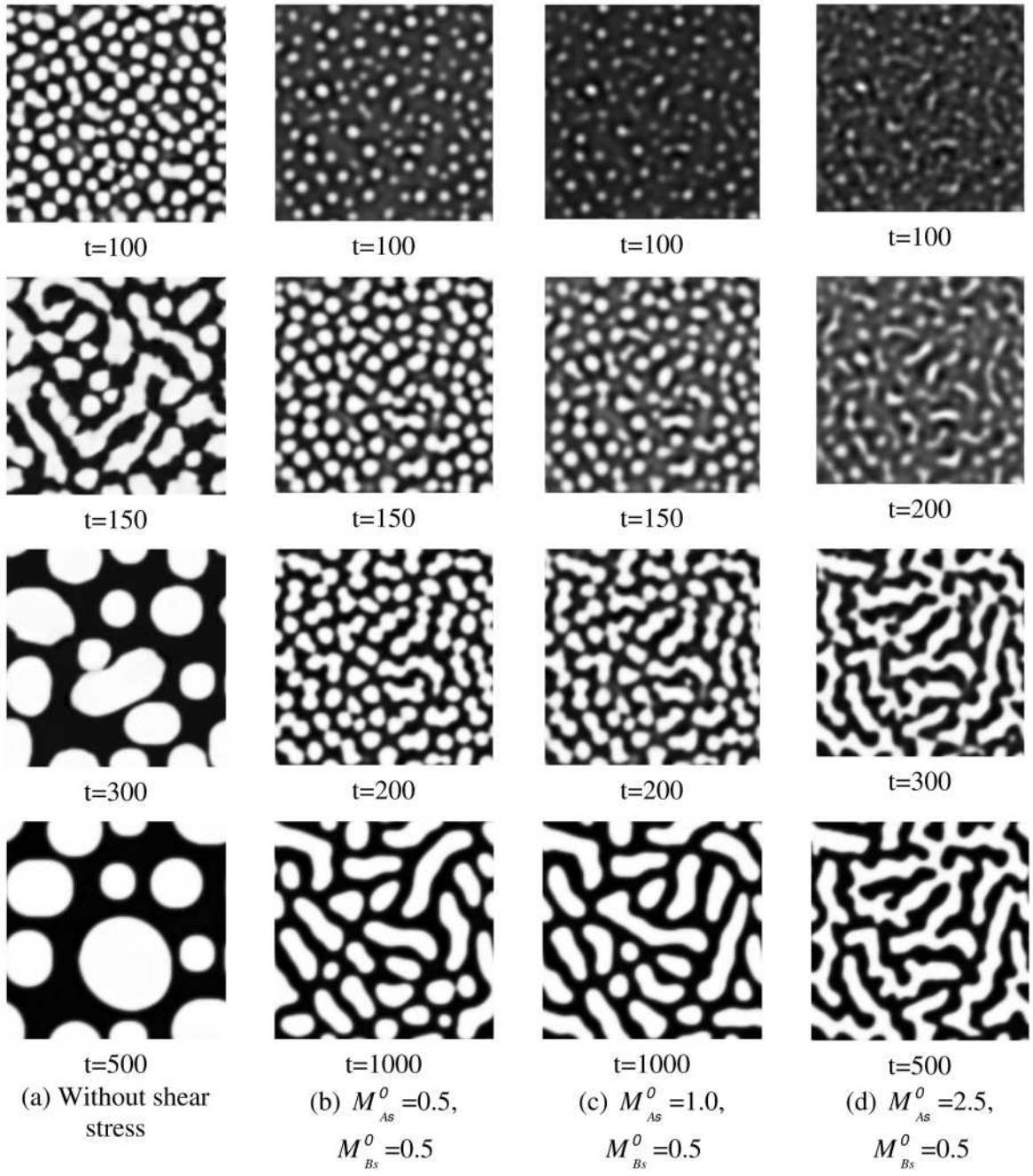

Fig. 5. Time evolution of phase-separating domains of polymer blends with shear modulus and for critical mixtures $\bar{\phi}_A = 0.5$. The parameters are set as $M^0_{Ab} = 2.5$, $M^0_{Bb} = 0.5$, $\tau^0_{As} = 50$; $\tau^0_{Bs} = 50$, $\tau^0_{Ab} = 10$; $\tau^0_{Bb} = 10$ and (a) without shear modulus, (b) $M^0_{As} = 0.5$, $M^0_{Bs} = 0.5$, (c) $M^0_{As} = 1.0$, $M^0_{Bs} = 0.5$, (d) $M^0_{As} = 2.5$, $M^0_{Bs} = 0.5$. A-rich regions and B-rich regions are represented by black and white, respectively.

that even without difference between shear moduli, the shear mechanical forces acting on different components are different for different bulk moduli. The component with higher bulk modulus bears a larger shear mechanical force. Comparing Figures 6b and c with Figure 6d, where different morphologies are observed, some features of the forces acting on the more viscoelastic A-rich phase in Figure 6d are: 1) the shear mechanical force is larger than the bulk mechanical force at the early stage of phase separation; 2) in the regimes after the force maxima the bulk mechanical force relaxes rapidly, but the shear mechanical force relaxes slowly, so a larger difference between these two forces is observed, resulting in the formation of the co-continuous structure.

Figure 7a shows the temporal change in the volume fraction of the more viscoelastic A-rich phase for the four cases shown in Figure 5. It can be seen that in the very early stage of phase separation, the homogeneous

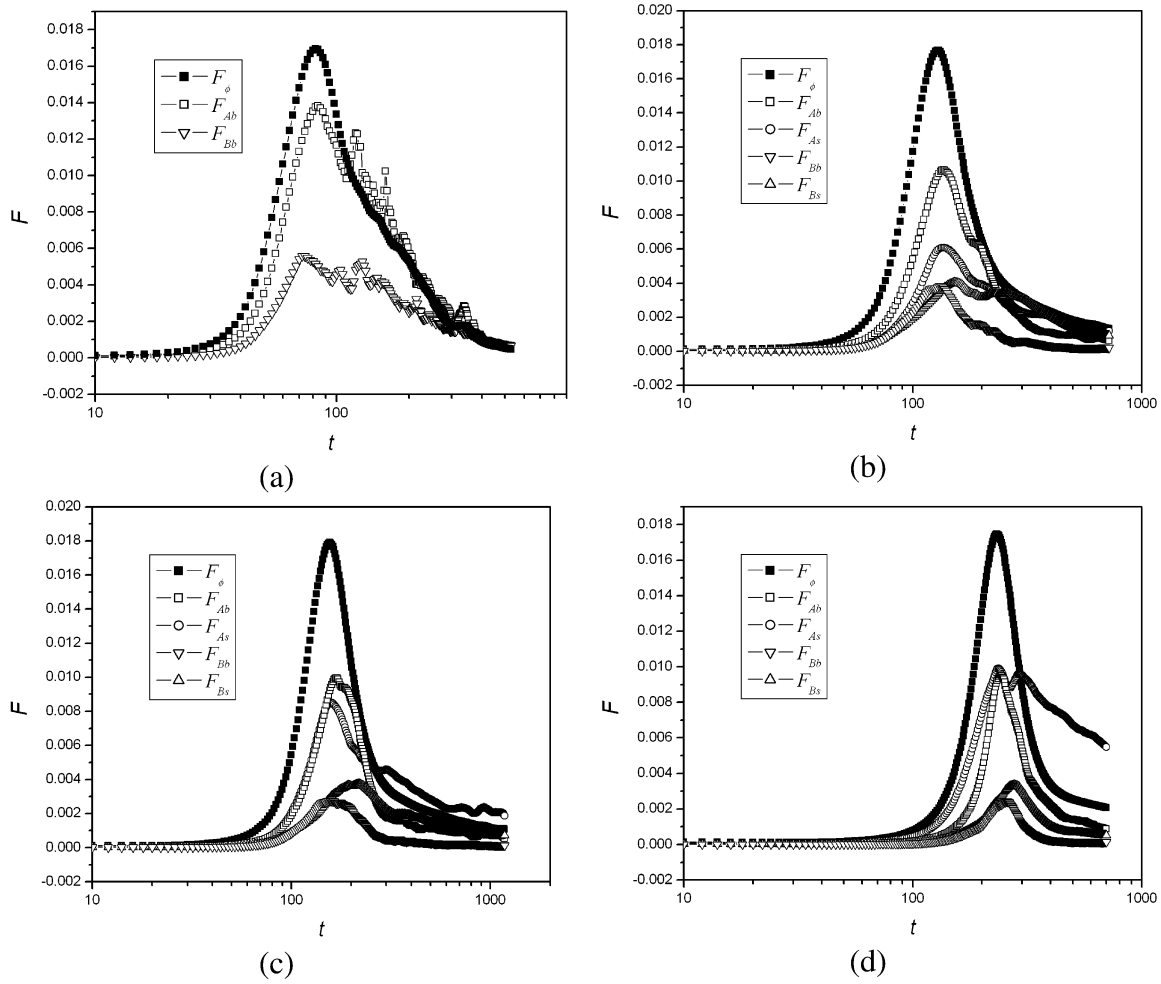

Fig. 6. Time evolution in the average magnitudes of thermodynamic, bulk and shear mechanical force for the cases depicted in Figure 5 (a), (b), (c) and (d).

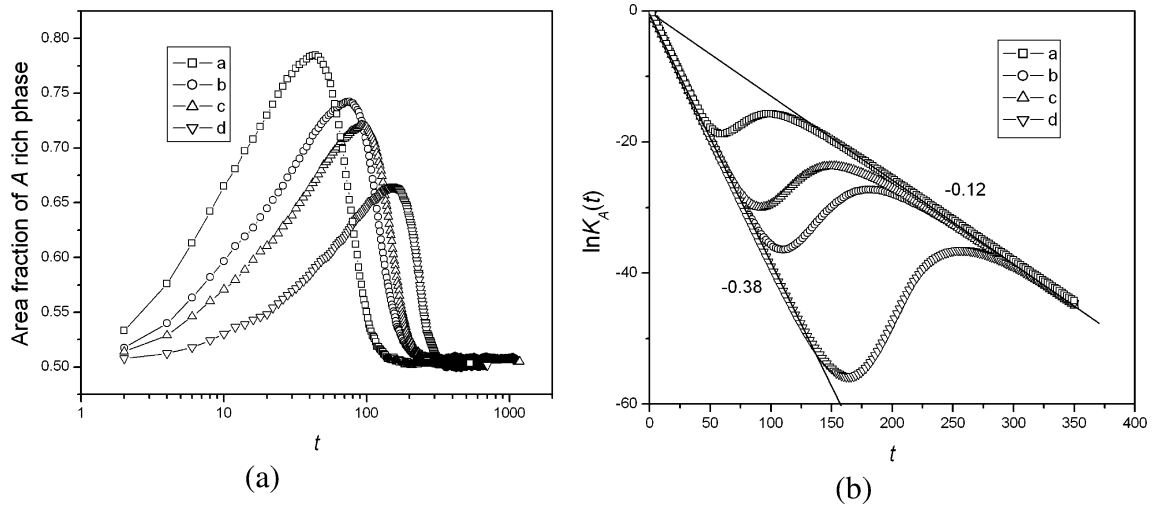

Fig. 7. (a) Time evolution in the area fraction of the A-rich phase for the cases depicted in Figure 5; (b) relaxation of the bulk modulus of the A-rich phase for the cases depicted in Figure 5.

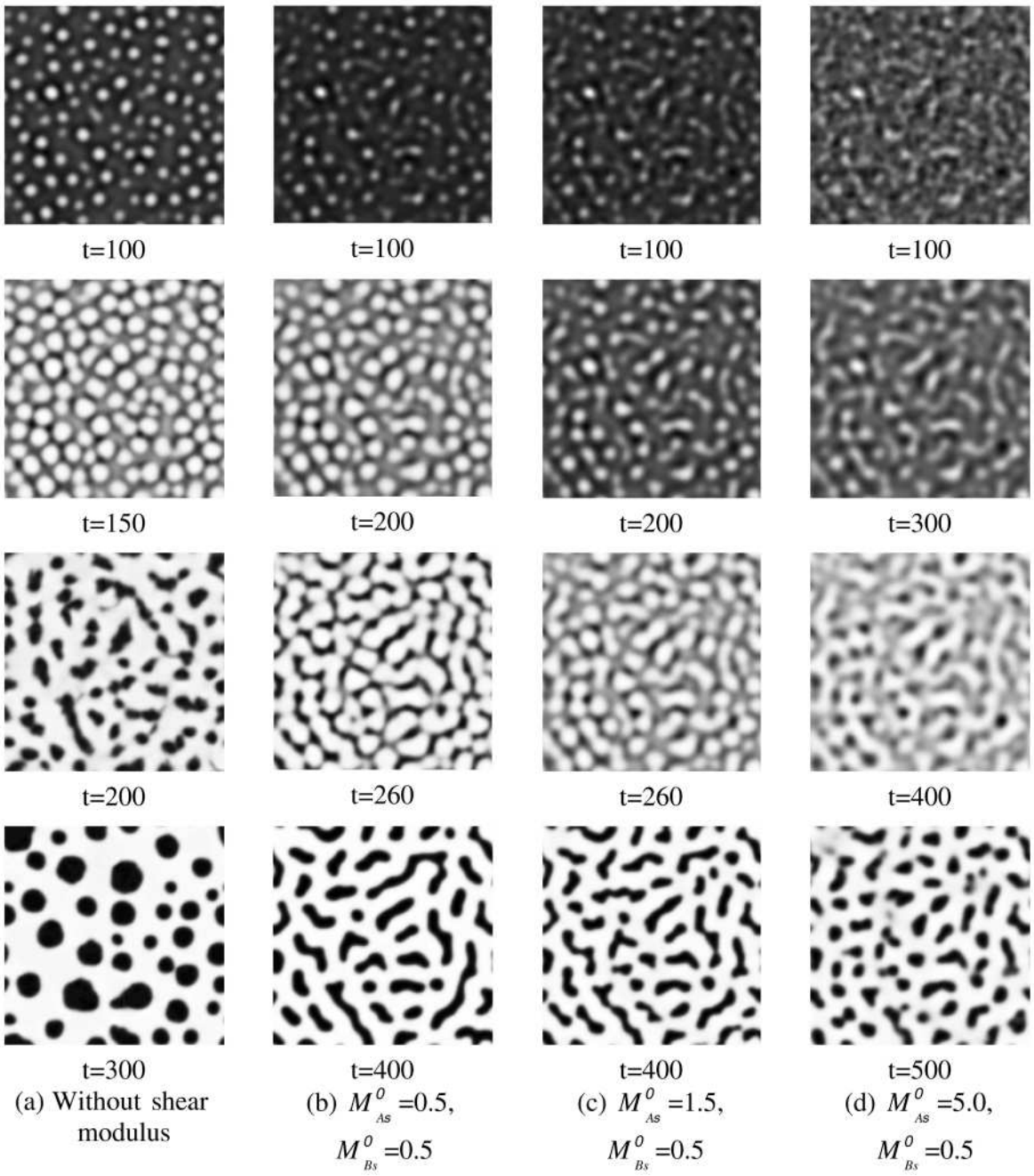

Fig. 8. Time evolution of phase-separating domains of polymer blends with bulk modulus and for off-critical mixtures $\bar{\phi}_A = 0.35$. The parameters are set as $M^0_{Ab} = 2.5$, $M^0_{Bb} = 0.5$, $\tau^0_{As} = 50$; $\tau^0_{Bs} = 50$,$\tau^0_{Ab} = 10$; $\tau^0_{Bb} = 10$ and (a) without shear modulus, (b) $M^0_{As} = 0.5$, $M^0_{Bs} = 0.5$, (c) $M^0_{As} = 1.5$, $M^0_{Bs} = 0.5$, (d) $M^0_{As} = 5.0$, $M^0_{Bs} = 0.5$. A-rich regions and B-rich regions are represented by black and white, respectively.

phase discharges the less viscoelastic phase due to the thermodynamic force and becomes the more viscoelastic phase resulting in an increase of the area of the more viscoelastic A-rich phase. Later, the less viscoelastic phase becomes larger and larger, resulting in a decrease of the area of the more viscoelastic A-rich phase. In the end, the area of the more viscoelastic A-rich phase reaches equilibrium value. Here, we should point out that without difference between bulk moduli, there is no change in the volume fraction. One important feature in Figure 7a is that with the increase of difference between shear moduli, the maxima of area fraction of more viscoelastic A-rich phase decrease, which indicates that the shear stress suppresses the formation of isolated droplets of the less viscoelastic B-rich component.

Figure 7b shows the temporal relaxation patterns of the bulk modulus of the A-rich phase for the four cases shown in Figure 5. There exist three regimes, including

two linear regimes and one transition regime. The first linear regime corresponds to the very early stage of phase separation, during which the concentration fluctuation is strongly suppressed and the less viscoelastic B-rich phase is about to emerge from the homogenous state. The second linear regime corresponds to the late stage of phase separation where the concentration fluctuations of the two phases reach their equilibrium value. The inverse relaxation time for the first linear region is much shorter than that for the second one and it has nothing to do with bulk and shear moduli. The inverse relaxation time for the first linear region is only related to quench depth and the bulk relaxation time $\tau^0_{A\mathrm{b}}$. The transition regime between two linear regimes corresponds to the intermediate stage of phase separation, during which the suppression of the concentration is gradually relieved and concentration fluctuations rapidly increase. Larger values of difference between shear moduli will result in longer retardation times.

3.2 Case of $\bar{\phi}_{\mathbf{A}} = 0.35$

If we only take account of shear stress, neglect the effect of the bulk stress and use the same parameters as in Figure 2, there is almost no morphological difference compared with Figure 1b. This is in agreement with Tanaka and Araki's simulation results [31] for polymer solutions. For simplicity, we do not show the morphological evolution here. Because the composition is far from critical, we can conjecture that morphological changes may need a very large difference between shear moduli.

Figure 8 shows the morphological evolution with the bulk modulus. The parameters are set as $M^0_{A\mathrm{b}} = 2.5$, $M^0_{B\mathrm{b}} = 0.5$, $\tau^0_{A\mathrm{s}} = 50$; $\tau^0_{B\mathrm{s}} = 50$, $\tau^0_{A\mathrm{b}} = 10$ and $\tau^0_{B\mathrm{b}} = 10$, which are the same as in Figure 5. For the case without shear modulus (Fig. 8a), the domains of the lower bulk modulus B-rich phase nucleate, grow up and seldom merge together, leading to the formation of the higher bulk modulus A-rich phase network, *e.g.*, $t = 150$, although the component A is the minority phase. With the increase of time, the network breaks up quickly and phase inversion is observed. If we change the shear moduli into $M^0_{A\mathrm{s}} = 0.5$, $M^0_{B\mathrm{s}} = 0.5$ (Fig. 8b) and $M^0_{A\mathrm{s}} = 1.5$, $M^0_{B\mathrm{s}} = 0.5$ (Fig. 8c), the pattern evolution is almost the same except that a networklike pattern can keep longer time and a networklike pattern composed of highly elongated thin structures is observed. We should point out that in Figure 8b, there is no difference between the shear moduli of the two components. This indicates that bulk stress is the precondition for the formation of a minority networklike phase and shear stress should be responsible for a networklike pattern composed of highly elongated thin structures. These results are consistent with Tanaka and Araki's simulation results [31] for polymer solutions. But if we further enhance $M^0_{A\mathrm{s}}$, *i.e.*, $M^0_{A\mathrm{s}} = 5.0$, $M^0_{B\mathrm{s}} = 0.5$, the higher bulk modulus A-rich phase network is not observed (Fig. 8d), because once the lower bulk modulus B droplets form, they are deformed under large shear stress. This is completely different from Tanaka and Araki's simulation results [31], where the shear modulus of the polymer is too small.

4 Conclusion

In this paper, we have investigated the dynamics and morphology of viscoelastic phase separation in polymer blends by the two-fluid model. At critical composition, we have re-checked the effect of shear moduli in the viscoelastic phase separation. The results show that in the intermediate stage of phase separation, the higher shear modulus phase forms obviously dispersed droplets and cylinders in the matrix of the lower shear modulus phase if the difference between the shear moduli of the two components is large enough. This result is opposite to the effect of bulk moduli where the higher bulk modulus A-rich phase forms a networklike pattern even if it is the minority phase. The morphological formation is determined by the competition of opposite effects between shear modulus and bulk modulus.

For polymer blends in critical composition, pure bulk modulus difference leads the higher bulk modulus A-rich phase to form a networklike pattern in the intermediate stage of phase separation, and it never relaxes to a co-continuous structure in the late stage of phase separation. If enough large difference between the shear moduli of the two components is introduced, instead of a networklike pattern, a co-continuous structure is observed, resulting from the competition.

For polymer blends in off-critical composition, the pure bulk modulus difference also leads the higher bulk modulus A-rich phase to form a networklike pattern in the intermediate stage of the phase separation, but phase inversion is observed rapidly. Small difference between the shear moduli of the two components can support a networklike pattern to keep for longer time. But due to the sufficiently large difference between shear moduli a networklike pattern cannot be observed.

The work received financial support by the SFB 428 of the "Deutsche Forschungsgemeinschaft".

References

1. J.D. Gunton, M.S. Miguel, P.S. Sahni, *Phase Transition and Critical Phenomena*, edited by C. Domb, J.H. Lebowitz, Vol. **8** (Academic, London, 1983).
2. P.C. Hohenberg, B.I. Halperin, Rev. Mod. Phys. **49**, 435 (1977).
3. A.J. Bray, Adv. Phys. **43**, 357 (1994).
4. H. Furukawa, Adv. Phys. **34**, 703 (1985).
5. I.M. Lifshitz, V.V. Slyozov, J. Phys. Chem. Solids **19**, 35 (1961).
6. J.W. Cahn, J.E. Hilliard, J. Chem. Phys. **28**, 258 (1958).
7. K. Luo, Y. Yang, Macromol. Theory Simul. **11**, 429 (2002).
8. P.G. De Gennes, J. Chem. Phys. **72**, 4756 (1980).
9. K. Binder, H.L. Frisch, J. Jackle, J. Chem. Phys. **85**, 1505 (1986).

10. P. Pincus, J. Chem. Phys. **75**, 1996 (1981).
11. K. Binder, J. Chem. Phys. **79**, 6387 (1983).
12. A. Onuki, J. Chem. Phys. **85**, 1122 (1986).
13. H. Tanaka, J. Phys. Condens. Matter **12**, 207 (2000).
14. H. Tanaka, Macromolecules **25**, 6377 (1992).
15. H. Tanaka, Phys. Rev. Lett. **71**, 3158 (1993).
16. H. Tanaka, Phys. Rev. Lett. **76**, 787 (1996).
17. D. Sappelt, J. Jackle, Physica A **240**, 453 (1997).
18. D. Sappelt, J. Jackle, Europhys. Lett. **37**, 13 (1997).
19. D. Sappelt, J. Jackle, Polymer **39**, 5253 (1998).
20. R. Ahluwalia, Phys. Rev. E **59**, 263 (1999).
21. N. Clarke, T.C.B. McLeish, S. Pavawongsak, J.S. Higgins, Macromolecules **30**, 4459 (1997).
22. Y. Cao, H. Zhang, Z. Xiong, Y. Yang, Macromol. Theory Simul. **10**, 314 (2001).
23. P.G. de Gennes, Macromolecules **9**, 587; 594 (1976).
24. F. Brochard, P.G. de Gennes, Macromolecules **10**, 1157 (1977); F. Brochard, J. Phys. (Paris) **44**, 39 (1983).
25. E. Helfand, G.H. Fredrickson, Phys. Rev. Lett. **62**, 2468 (1989).
26. A. Onuki, Phys. Rev. Lett. **62**, 2427 (1989); J. Phys. Soc. Jpn. **59**, 3423 (1990).
27. M. Doi, A. Onuki, J. Phys. II **2**, 1631 (1992).
28. S.T. Milner, Phys. Rev. E **48**, 3674 (1993).
29. T. Taniguchi, A. Onuki, Phys. Rev. Lett. **77**, 4910 (1996).
30. H. Tanaka, T. Araki, Phys. Rev. Lett. **78**, 4966 (1997).
31. T. Araki, H. Tanaka, Macromolecules **34**, 1953 (2001).
32. H. Tanaka, Phys. Rev. E **56**, 4451 (1997).
33. H. Tanaka, T. Koyama, T. Araki, J. Phys. Condens. Matter **15**, S383 (2003).
34. J. Zhang, Z. Zhang, H. Zhang, Y. Yang, Phys. Rev. E **64**, 051510 (2001).
35. Y. Huo, H. Zhang, Y. Yang, Macromolecules **36**, 5383 (2003).
36. P.G. de Gennes, *Scaling Concepts in Polymer Physics* (Cornell University Press, New York, 1979).
37. J. Zhu, L.Q. Chen, J. Shen, V. Tikare, Phys. Rev. E **60**, 3564 (1999).